



Tartaruga, I., Cooper, J. E., Georgiou, G., & Khodaparast, H. (2017). Flutter uncertainty quantification for the S4T model. In *55th AIAA Aerospace Sciences Meeting* American Institute of Aeronautics and Astronautics Inc. (AIAA). <https://doi.org/10.2514/6.2017-1653>

Peer reviewed version

Link to published version (if available):
[10.2514/6.2017-1653](https://doi.org/10.2514/6.2017-1653)

[Link to publication record in Explore Bristol Research](#)
PDF-document

This is the author accepted manuscript (AAM). The final published version (version of record) is available online via AIAA at <https://arc.aiaa.org/doi/abs/10.2514/6.2017-1653>. Please refer to any applicable terms of use of the publisher.

University of Bristol - Explore Bristol Research

General rights

This document is made available in accordance with publisher policies. Please cite only the published version using the reference above. Full terms of use are available:
<http://www.bristol.ac.uk/red/research-policy/pure/user-guides/ebr-terms/>

Flutter Uncertainty Quantification for the S4T Model

I Tartaruga¹, J.E. Cooper²
University of Bristol, Bristol, BS8 1TH, United Kingdom

G. Georgiou³,
University of Liverpool, Liverpool, United Kingdom

H.H. Khodaparast⁴
Swansea University, Swansea, United Kingdom

Abstract submitted for the Special SCITECH session on AVT Uncertainty Quantification

The application of uncertainty analysis, including probabilistic and non-probabilistic approaches, to the prediction of the dynamic pressure at which flutter occurs is considered for the S4T Semi-Span Super-Sonic Transport wind-tunnel model. A SVD based reduced order modelling approach, along with the Polynomial Chaos Expansion and Fuzzy Analysis methods for uncertainty quantification, are described and used to explore the effects that variations in the structural mass, resembling variations in the fuel load, have on the linear flutter analyses for a range of subsonic and supersonic speeds. All the approaches are able to efficiently quantify the effects of structural uncertainty on the aeroelastic behavior.

I. Introduction

Supersonic flight for civil aircraft has been of interest since the 1960s when several supersonic commercial airline projects started, and eventually the Anglo-French Concorde and the Russian Tupolev Tu-144 entered into service. Political, environmental and economic issues hindered the commercial running of these aircraft, and Concorde was withdrawn from service in 2003. There are a wide range of technical challenges that impede the development of supersonic passenger aircraft including: noise, cruise efficiency, sonic boom modeling, high altitude emissions and durability at high temperatures, and thus there are currently no supersonic commercial configurations being developed. It is odd that, unlike the last three decades of the 20th century, it is not possible nowadays for paying passengers to cross the Atlantic by air at supersonic speeds. In order to enable supersonic aircraft to utilize their full capability and overcome technical and financial barriers, a detailed investigation is required.

In the mid- to late-1990s, the NASA High Speed Research (HSR) program undertook research in the areas of computational and experimental aeroelasticity to investigate supersonic flight. Several aeroelastic wind-tunnel models were designed, manufactured and tested; in order to investigate experimentally the aeroelastic behavior of the Technology Concept Aircraft (TCA), an aeroelastically scaled semi-span wind-tunnel model was designed, called the Semi-Span Super-Sonic Transport (S4T) [1]. Following this work, the Supersonics Project was established in 2006 under the NASA Fundamental Aeronautics Program in which the Aeroservoelasticity (ASE) Element was tasked with the modeling, analysis, and prediction of aeroelastic and ASE phenomena associated with supersonic configurations.

The S4T wind-tunnel model was the subject of four wind-tunnel tests in the Transonic Dynamics Tunnel (TDT): two open-loop (no feedback control) tests and two closed-loop (with feedback control) tests, between 2007 and 2010 [1]. The goals of the open-loop tests were to acquire system identification data to enable the design of ASE control laws. The goals of the closed-loop tests were to evaluate several candidate ASE control laws in the performance of gust load alleviation (GLA), ride quality enhancement (RQE), and flutter suppression (FS) looking at both independent and combined functions. The S4T model provided a sophisticated test-bed for developing multi-disciplinary numerical and experimental capabilities for supersonic aircraft and is a scaled semi span wind-tunnel

¹ PhD Student, Dept. of Aerospace Engineering

² Airbus Royal Academy of Engineering Sir George White Professor of Aerospace Engineering, AFAIAA

³ Senior Research Engineer, Virtual Engineering Centre

⁴ Lecturer in Aerospace Engineering, College of Engineering

model, equipped with three active surfaces (ride control vane, aileron and horizontal tail) and flow-through nacelles with flexible mounts [1].

The importance in considering and quantifying the presence of uncertainty due to variations in the structure, materials, aerodynamic characteristics and control system in the design of aerospace structures, as well as in a wide range of other scientific fields, has recently become recognized; however, the presence of uncertainty increases the complexity and computational requirements of the analysis. There are several previous applications of uncertainty analysis in the aeronautical field, concerning critical conditions due to loads [2-5] and self-induced oscillations such as shimmy [6-7] and flutter [8-14]. Initial uncertainty quantification (UQ) studies relating to the S4T model can be found in references [14] and [15].

This work considers the uncertainty quantification of the flutter analysis of the S4T wind tunnel model. A range of different methodologies (Singular Value Decomposition (SVD) based technique, Polynomial Chaos and a Fuzzy Logic based methodology) are applied to data generated from tightly coupled numerical models (Finite Element and Doublet Lattice aerodynamic codes) in order to demonstrate their effectiveness in assessing the uncertainty of the flutter analysis subject to variations in some of the structural parameters.

II. S4T MODEL and PARAMETER UNCERTAINTY

The Semi-Span Super-Sonic Transport vehicle (S4T) is an aeroelastically-scaled wind-tunnel model of a cruise aircraft, designed and constructed at NASA Langley in order to conduct transonic experimental and numerical studies related to gust alleviation, ride quality, flight dynamics and propulsion. Figure 1 shows the physical and finite element model displaying the three active surfaces (ride-control vane, wing aileron and all-movable horizontal tail), the engine nacelles, the flexible fuselage beam and wing [14].

Uncertainties of the fuselage and engine masses were considered in this work. In particular, the uncertainty has been described considering 5 scale factors applied to groups of concentrated masses:

1. 11 concentrated masses along the flexible fuselage
2. 4 groups of concentrated masses at engine nacelles (inboard and outboard engines): 2 groups of 8 and 15 concentrated masses per each engine

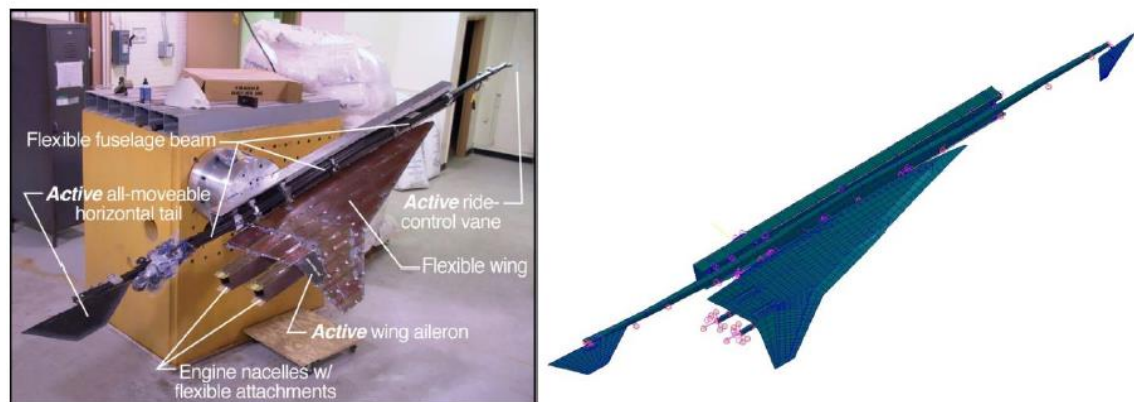


Figure 1: S4T model.

A. Singular Value Decomposition Based Method

A Singular Value Decomposition (SVD) based method [2,3] was used to quantify the system uncertainty, describing probabilistically the flutter pressure dynamic trend with Mach number changes, and also identifying the worst case scenario. The method is summarized in Figure 2 and explained in the following.

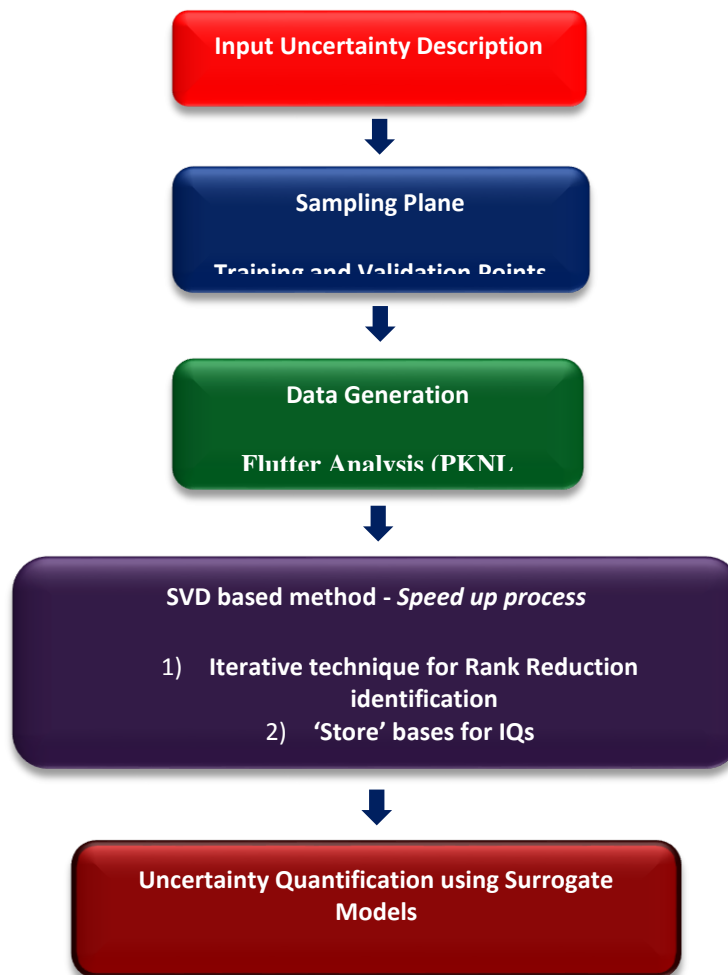


Figure 2: Flow chart of the SVD Based ROM Approach

Step 1 - Probabilistic Parameter Variation

The input uncertainties, varying the concentrated masses in the finite element model, were described in a probabilistic manner. A normal distribution was adopted for each mass and, as proposed in [14], coefficients of variation of 0.1 and 0.3333 were selected to scale the groups of concentrated masses at the flexible fuselage and engine nacelles, respectively. The engine nacelle mass variation was very high and thus a limitation in terms of the cumulative density function (CDF) was considered; maximum and minimum values of (0.905, 0.095) and (0.7, 0.3) were considered for the CDF related to the flexible fuselage and nacelles.

Step 2 - Sampling of Data

Initially, the sampling plane to be considered for the generation of interested quantities (IQs), is defined. A suitable sampling method (e.g. Latin Hypercube Sampling, Hamilton or Sobol sequences) is selected and the IQs determined for three types of sampling points, using the numerical model that best represents the analysed problem. Here, the IQ is the flutter dynamic pressure and the Latin Hypercube Sampling method was adopted. The sampling points are:

- training points, which are used to train surrogate models adopted to speed up the Uncertainty Quantification (UQ)
- validation points for the surrogate models, which are needed to validate the trained surrogate models

- validation points for the results given by the UQ, which are used to obtain an 'actual' but time consuming UQ

The 'actual' UQ is performed using Monte Carlo Simulations (MCS) analysis. There would be no benefit in performing this last step in practice due to computational limitations and it would also negate the reason for developing these methodologies.

Step 3 – Flutter Dynamic Pressure Identification

The identification of the flutter dynamic pressure was performed using the PKNL method [16]. The flutter analysis was computed for different sets of Mach numbers and velocities and, for each set, the density ratio ρ was changed until a change in the sign of the damping ratio (c) of one mode occurs. The flutter analysis is iterative and considers a set of values for the density ratio for each selected set of Mach number and velocity. A linear interpolation was used between the two sets of density and damping ratio (ρ_i, c_i $i = 1, 2$) for which a change of the sign of the damping ratio occurs; the value of the density at flutter occurrence, ρ_F is approximated as

$$\rho_F \cong -c_2 \cdot \frac{\rho_1 - \rho_2}{c_1 - c_2} + \rho_2 \quad (1)$$

and the flutter dynamic pressure q_F is given by

$$q_F = \frac{1}{2} \rho_F V^2 \quad (2)$$

Step 4 - Generation of Data Matrix

Once the data of interest has been generated, in this case the flutter speed for given mass variation and Mach numbers, a data matrix is constructed from the values of the flutter dynamic pressure related to the training points. The SVD can then be applied for feature extraction [2-7]. The matrix defined for the flutter dynamic pressure has as many rows as the number of parameter variations (e.g. concentrated masses) (D) and as many columns as the number of Mach considered in the flutter analysis (B). A SVD is applied to the data matrix A using the training data such that

$$\mathbf{A} = \mathbf{U} \mathbf{\Sigma} \mathbf{V}^T \quad (3)$$

The rank of the data matrix \mathbf{A} (and so of the model order) is reduced by selecting the most significant singular values in $\mathbf{\Sigma}$. The product of the reduced 'singular values matrix' $\mathbf{\Sigma}_k$ and the transpose of the 'right singular vector matrix' \mathbf{V}_k^T is adopted as the "basis" and this is assumed to remain constant over the considered parameter variation range. A surrogate model is then constructed for each column of the reduced 'left singular vector matrix' \mathbf{U}_k . For any desired set of parameter values, a time history can be reconstructed by multiplying the basis $\mathbf{\Sigma}_k \mathbf{V}_k^T$ by the surrogates of \mathbf{U}_k evaluated at the selected parameter values. The surrogates can then be used to perform the uncertainty quantification. Figure 3 shows the formulation of data matrix A and its decomposition into the three sub-matrices (U, Σ , V); clarifying how the surrogate models are developed for the analyzed problem.

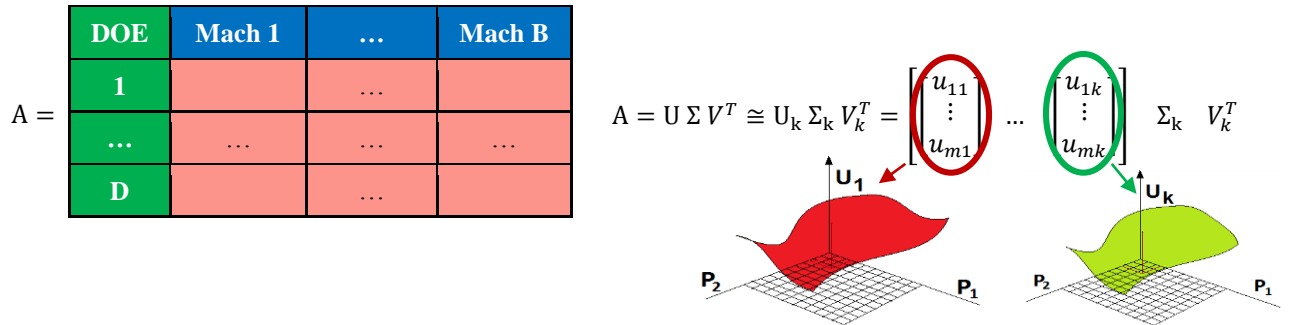


Figure 3: Data Matrix Formulation

In order to speed up the process, the terms to be retained are identified by fixing the maximum acceptable error caused by the rank reduction. Once this error is chosen, the energy ‘captured’ by the reduced matrix and the singular values to be retained can be identified. This energy is linked with the Frobenius norm and is determined by using the captured energy criterion to identify the required amount of rank reduction. The energy captured criterion consists of selecting enough singular values of the matrix of interest, such that the sum of their squares is a certain percentage t of the total sum of the squared values. Such an approach has given very encouraging results on previous examples. In this work, the singular values (surrogate models) characterizing the SVD are automatically obtained once the maximum acceptable error is defined. However, the percentage $t\%$ that should be taken as the threshold is problem dependent and is often difficult to know a-priori.

The authors have considered an iterative procedure shown in Figure 4, where the number of singular values is increased, and so the percentage $t\%$, and the rank reduction updated until the desired maximum error is met. The Mean Average Percentage Error (MAPE) [2-7] is considered here with the average being taken in terms of all the considered training points. Once the sampling plane for the training has been defined and the rank reduction selected with the procedure presented above, $\Sigma_k V_k^T \in \mathbb{R}^{k \times n}$ is considered as a basis which is assumed not to change throughout the design space.

The dynamic pressure at flutter is the IQ and the variation in terms of five groups of concentrated masses were considered. It is recommended to consider different surrogate models and to evaluate the one that performs best using the responses obtained at the validation points. In the present analysis, the Blind Kriging methodology is adopted since it is particularly good at dealing with a Gaussian process. Although such as approach is still “supervised learning”, the ‘training data is harnessed in a subtler way’ [17] and good performance has been found in the presence of strong trends [18]

Step 5 – Uncertainty Propagation

Having identified the basis and surrogate models to be used with the SVD based method, the uncertainty in the system can be propagated without recourse to the full numerical model, thereby saving computational time but still obtaining a high accuracy. This aim is accomplished here by constructing a 5D sampling plane (five scaled factors were adopted) with an arbitrary high number of data points and evaluating the trained surrogate models for all the considered set of points. Then the flutter dynamic pressure at the i th point in the defined sampling plane is determined for all the selected Mach numbers and velocities multiplying the row of surrogate models $[u_{i1} \dots u_{ik}]$ by the previously determined basis $\Sigma_k V_k^T$.

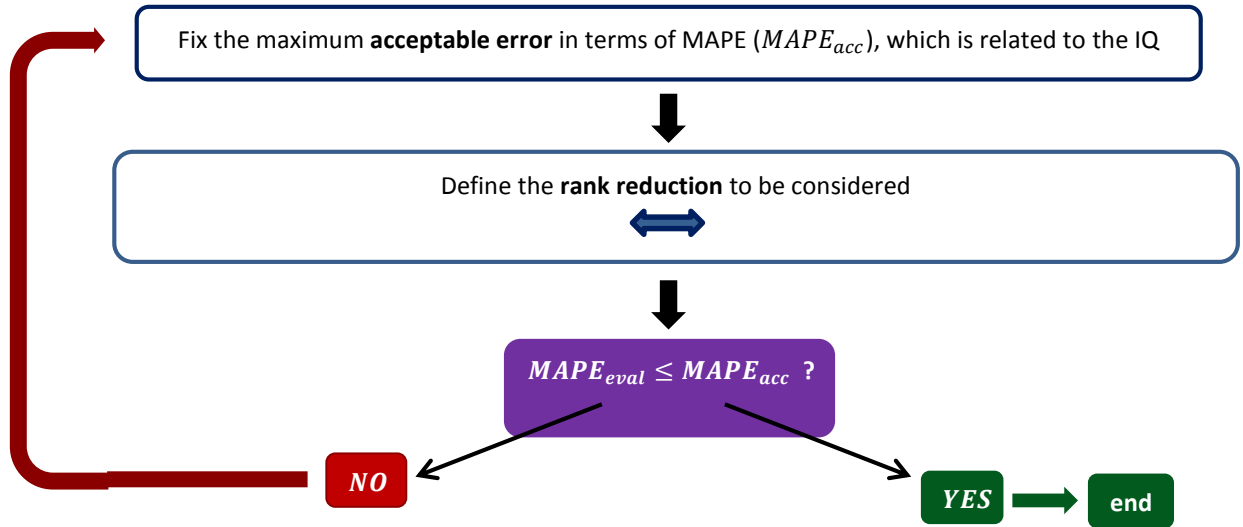


Figure 4: Iterative technique for Rank Reduction identification. $MAPE_{eval}$ and $MAPE_{acc}$ are the mean average percentage errors obtained having fixed the rank reduction and defined as acceptable, respectively.

For each value of Mach and velocity, a statistical description for the flutter dynamic pressure can be depicted using the Matlab function *ksdensity* and values of the flutter dynamic pressure for fixed quantiles can be obtained using the Matlab function *quantile*. The worst case scenario and the relative bounds for the flutter dynamic pressure can be

dealt with by considering the quantiles equal to 0 and 1. A major advantage of the developed method is the possibility to reduce the computational time required by a Monte Carlo Simulation (MCS) and completely identify the configurations (e.g. concentrated mass) for which the flutter occurs whilst still maintaining a good accuracy.

B. Polynomial Chaos Expansion

Stochastic expansion techniques, such as Polynomial Chaos Expansion (PCE) and Stochastic Collocation (SC), expand the output response in a series of random variables for uncertainty quantification and propagation with reduced computational effort. The development of the stochastic expansions started when Wiener [19] introduced a mathematical model, in an effort to describe the irregularities appeared in Brownian motion using a multiple stochastic integral with homogeneous chaos. Ito [20] then modified Wiener's work and showed that any stochastic process can be described as a Wiener process. Ghanem and Spanos [21] defined a simple definition of the PCE as a convergent series of the form

$$u = a_0 H_0 + \sum_{i=1}^{\infty} a_i H_1(\zeta_i) + \sum_{i=1}^{\infty} \sum_{i_2=1}^{i_1} a_{i i_2} H_2(\zeta_i, \zeta_{i_2}) + \sum_{i=1}^{\infty} \sum_{i_2=1}^{i_1} \sum_{i_3=1}^{i_2} a_{i i_2 i_3} H_3(\zeta_i, \zeta_{i_2}, \zeta_{i_3}) + \dots, \quad (4)$$

where $\{\zeta_i\}_{i=1}^{\infty}$ represents a set of independent stochastic Gaussian variables, $H_p(\zeta_1, \dots, \zeta_{i_p})$ is a set of multidimensional Hermite polynomials of order p and a_1, \dots, a_{i_p} are properly defined coefficients. The approximation of the output response u can be rewritten using different orthogonal polynomials which belong to the Askey scheme, such as the Laguerre, Jacobi and Legendre if the input random variables follow the gamma, beta and uniform distributions respectively.

In the present study, the uncertain parameters $\{\zeta_i\}_{i=1}^{\infty}$ were defined as normalized variables using expression

$$\zeta_i = \frac{x_i - \mu_i}{\sigma_i}, \quad (5)$$

where μ_i and σ_i^2 represent the mean value and the variance of the i th random variable. The Hermite polynomials with respect to the independent variable ζ are defined by

$$H_0(\zeta) = 1, \quad H_1(\zeta) = \zeta, \quad H_2(\zeta) = \zeta^2 - 1, \quad H_3(\zeta) = \zeta^3 - 3\zeta, \quad H_4(\zeta) = \zeta^4 - 6\zeta^2 + 3, \quad \dots \quad (6)$$

and, as a result, in the case of a single input parameter, the Polynomial Chaos Expansion analytical formula truncated at the fourth order is written as

$$u = a_0 + a_1 \zeta + a_2 (\zeta^2 - 1) + a_3 (\zeta^3 - 3\zeta) + a_4 (\zeta^4 - 6\zeta^2 + 3), \quad (7)$$

whereas in the case of two uncertain variables, ζ_1, ζ_2 the second order stochastic expansion is obtained as

$$u = a_0 + a_1 \zeta_1 + a_2 \zeta_2 + a_3 (\zeta_1^2 - 1) + a_4 \zeta_1 \zeta_2 + a_5 (\zeta_2^2 - 1). \quad (8)$$

The unknown coefficients a_i of the Polynomial Chaos Expansions can be calculated using a regression analysis or the statistically averaging method. Here, a linear regression process was used and the polynomial coefficients were predicted by solving the following system of equations for the case of a single uncertain variable such that

$$\begin{bmatrix} u_1 \\ \vdots \\ u_n \end{bmatrix} = \begin{bmatrix} H_{01} & H_{11} & \dots & H_{p1} \\ H_{02} & H_{12} & \dots & H_{p2} \\ \vdots & \vdots & \vdots & \vdots \\ H_{0n} & H_{1n} & \dots & H_{pn} \end{bmatrix} \begin{bmatrix} a_0 \\ a_1 \\ \vdots \\ a_p \end{bmatrix}, \quad (9)$$

where the term u_i for $i=1,\dots,n$ is a discrete observation of the output response, while the element H_{pi} represents the value of the p -th order Hermite polynomial calculated for the i th value of the input parameter. The minimum sample size, needed for the calculation of the coefficients a_i , is defined as

$$n = \frac{(p+d)!}{p!d!}, \quad (10)$$

where d is the number of independent variables. Indicatively, the scalability of the minimum sample size with respect to the dimensionality of the problem and the order of the approximation polynomials is presented in Table 1.

Table 1: Minimum sample size for the regression analysis needed for the Polynomial Chaos Expansion approximation models.

| N | p=1 | p=2 | p=3 | p=4 |
|----------|----------|----------|----------|----------|
| d=1 | 2 | 3 | 4 | 5 |
| d=2 | 3 | 6 | 10 | 15 |
| d=3 | 4 | 10 | 20 | 35 |
| d=4 | 5 | 15 | 35 | 70 |
| \vdots | \vdots | \vdots | \vdots | \vdots |
| d=15 | 16 | 136 | 816 | 3876 |

In this case where the size of the observations is larger than the minimum, the system of equations described in Eq. (8) is over-determined and is solved using the least square approach. The accuracy of the regression coefficients depends upon the quantity and the quality of the obtained observations and for this reason, an efficient sampling technique, such as the Latin Hypercube method, which ensures that the points of the input variables are selected with equal probability, is necessary. After the evaluation of the unknown coefficients, the Polynomial Chaos Expansion models can be emulated for given values of the uncertain parameters and predict statistical properties of the output response, such as the mean value, the standard deviation and the probability density function at low computational cost.

C. Fuzzy Analysis

The Fuzzy logic concept was first introduced by Zadeh [22] and it is considered as a generalization of the classical (crisp) set. A brief description of fuzzy variable is provided in this chapter and we refer the reader to [23 – 27]. In the classical theory, a set consists of elements with membership values of either zero or one; a membership value of one indicates that the element belongs to the set, whereas zero membership value shows that the element does not belong to the set.

The fuzzy set \tilde{A} is defined as

$$\tilde{A} = \left\{ \zeta, \mu_{\tilde{A}}(\zeta) \mid \zeta \in \Psi, \mu_{\tilde{A}}(\zeta) \in [0, 1] \right\}. \quad (11)$$

where the membership function $\mu_{\tilde{A}}(\zeta)$ indicates the degree to which each element belongs to this set and varies within the range of 0 to 1. ζ is definitely a member if $\mu_{\tilde{A}}(\zeta) = 1$ and is a non-member if $\mu_{\tilde{A}}(\zeta) = 0$. For any intermediate case $0 < \mu_{\tilde{A}}(\zeta) < 1$ the membership is uncertain. This definition is required if a clear distinction between membership or exclusion of the members of the set is not possible.

Figures 5(a) and (b) show examples for the representation of fuzzy membership functions. Figure 5(a) shows the fuzzy variable with triangular membership function and as it can be seen, the interval model of an uncertain parameter can be interpreted within the definition of the crisp set theory. Thus, the uncertain parameter ζ which is represented by interval model is defined as

$$\zeta = \left[\underline{\zeta}, \bar{\zeta} \right], \quad (12)$$

where $\underline{\xi}$ and $\bar{\xi}$ are upper and lower bounds of uncertain variable ξ . In this definition, any value of ξ between upper and lower bounds ($\underline{\xi} \leq \xi \leq \bar{\xi}$) has membership value of one and those which are outside of this range ($\xi < \underline{\xi}$ and $\xi > \bar{\xi}$) have zero membership function.

The interval model is said to be non-possibilistic since no assumption is made regarding the probability distribution of uncertain parameter. Under the possibilistic interpretation of fuzzy sets and using the min-operator as t-norm [28,29], fuzzy variables are becoming a generalization of interval variables. In this context, the α -cuts of a fuzzy set play a crucial role in the computational and analytical methods involving fuzzy sets. As it can be seen in Figure 5(c), a α -cut interval is the set of realization with membership function value greater than α :

$$\xi_a = \{\xi \mid \mu_\xi \leq \alpha\}, \quad (13)$$

where ξ_a is an interval variable with lower bound of $\underline{\xi}_a$ and upper bound of $\bar{\xi}_a$. The Gaussian distribution can be approximated with a triangular membership function as depicted in Figure 5(d) [30]. The idea is to simply equate the area under the normalised Gaussian distribution function with the area under a triangular membership function, resulting in the approximation of the triangular fuzzy membership function defined as

$$\mu(\xi) = \max \left\{ 0, 1 - \frac{|\xi - m_\xi|}{\delta} \right\}, \quad (14)$$

where $\delta = \sqrt{2\pi}\sigma_\xi$, m_ξ and σ_ξ are the mean and standard deviation of the equivalent Gaussian distribution.

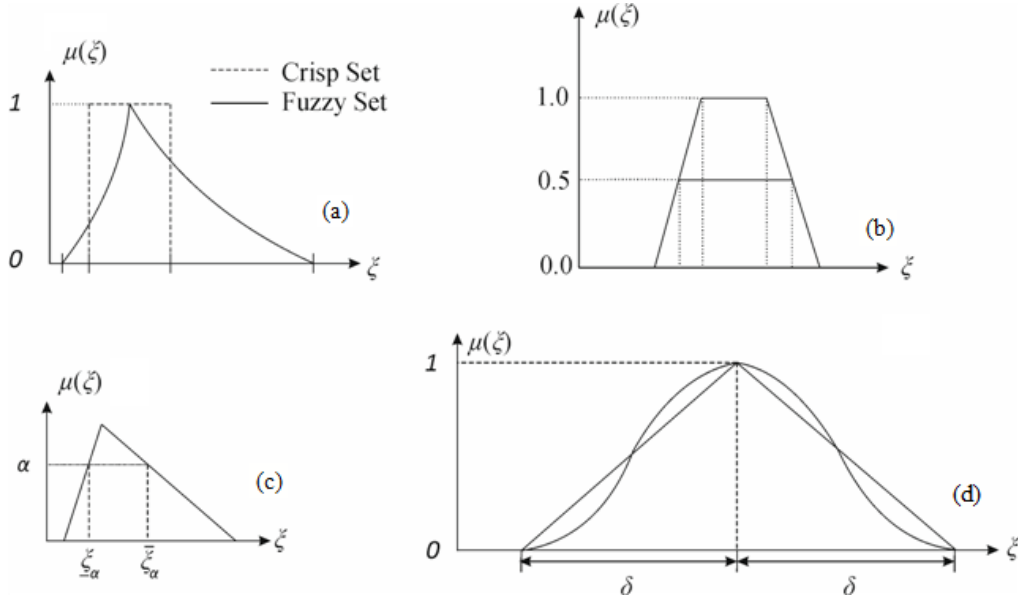


Figure 5. Examples of fuzzy membership functions: (a) triangular membership function, (b) trapezoidal membership function and (c) linear approximation of a Gaussian distribution by triangular fuzzy number (after [30]).

Once the membership functions of the uncertain input parameters of the aeroelastic system are defined, the fuzzy membership function of the system outputs can be calculated, for instance using the α -cuts procedure. In this case, the fuzzy analysis involves the application of interval analysis at a number of α -levels as illustrated in Figure 6. If each component of the response vector is represented by $u_i(\xi)$, the interval analysis at each α -cut is a numerical procedure equivalent to solving the following equation

$$\bar{u}_i = \max(u_i(\xi_a)) \text{ and } \underline{u}_i = \min(u_i(\xi_a)) \text{ with } i = 1, 2, \dots, n \quad (15)$$

subject to:

$$\underline{\xi}_a \leq \xi_a \leq \bar{\xi}_a.$$

Methods applicable for interval analysis, such as classical interval arithmetic [31], affine analysis [32,33] or vertex theorems [34] can be used. The Neumann expansion [35], the transformation method [30,36,37] and more recently, response surface based methods [34,38,39] have also been proposed for fuzzy uncertainty propagation. Among the existing methods, optimization methods are found to be the most accurate one in fuzzy propagation analysis [26,40]. At each α -level two optimization studies are carried out to find the bounds of output in Eq. (15). The Kriging predictor can be used to speed up the optimization procedure; in particular, once the Kriging model is constructed, the optimization studies needed at each α -level can be carried out rapidly using the surrogate model of the aeroelastic system.

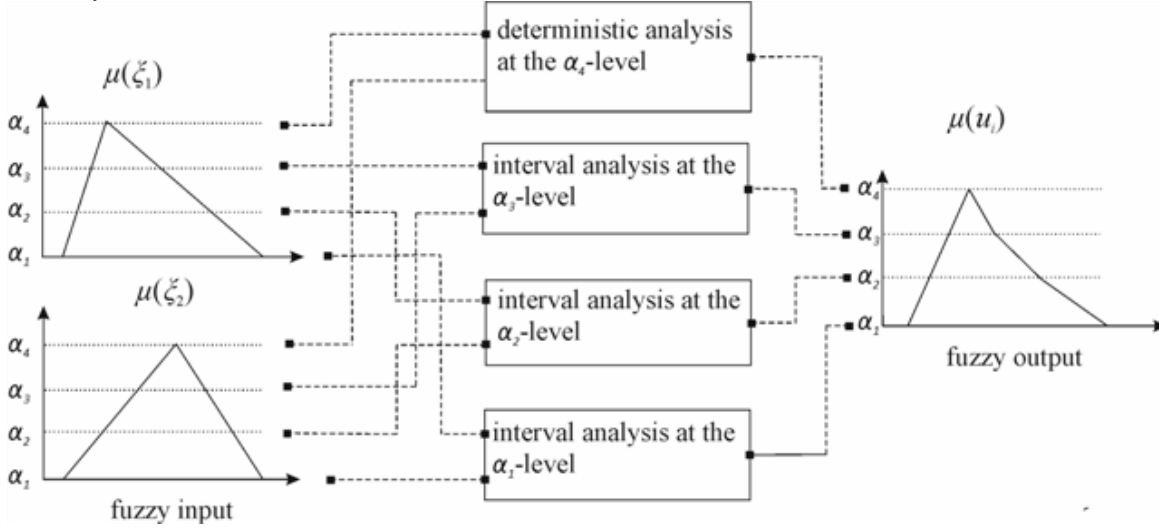


Figure 6 6-Level strategy, with 4 levels, for a function of two triangular fuzzy parameters (after [27]).

III. Uncertainty Quantification

Uncertainty quantification (UQ) of the effect of changes to the baseline system on the flutter speed were assessed for the SVD, Polynomial Chaos and Fuzzy Logic approaches. In all cases comparison is made with Monte-Carlo simulations which can be considered to be “truth”.

A. UQ Using SVD Approach

Figures 7 and 8 shows the results obtained using the SVD based surrogate approach. 1000 sampling points were considered to perform the uncertainty propagation. The validation of the uncertainty quantification was done using Monte Carlo Simulation (MCS). Validation of the resulting surrogate models shows a MAPE of less than 0.55%, with the exception of the results obtained for $M=1.1$. As stated before, this corresponds to the point with poor convergence for the PKNL method. For the sake of clarity and completeness, Table 4 shows all the evaluated MAPEs for all Mach numbers and quantiles. The accuracy is similar for both the considered training set of points; there is a slight improvement in the accuracy in terms of the probability density function if 200 training points were selected, as shown in Figure 9.

In addition, the SVD method requires much less computation than MCS. For the analyzed problem, using a desktop PC, the MCS takes about five days to propagate the uncertainty, whereas the SVD approach requires about 8 hours both to train all the surrogate models and propagate the uncertainty. Therefore, a reduction of approximately 95% in computation time was found.

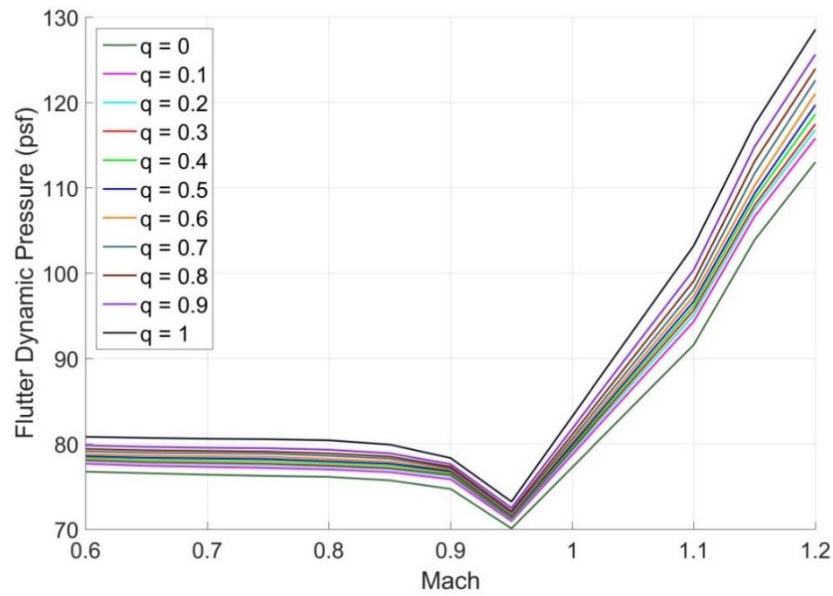


Figure 7: UQ quantile bounds using the SVD based technique.

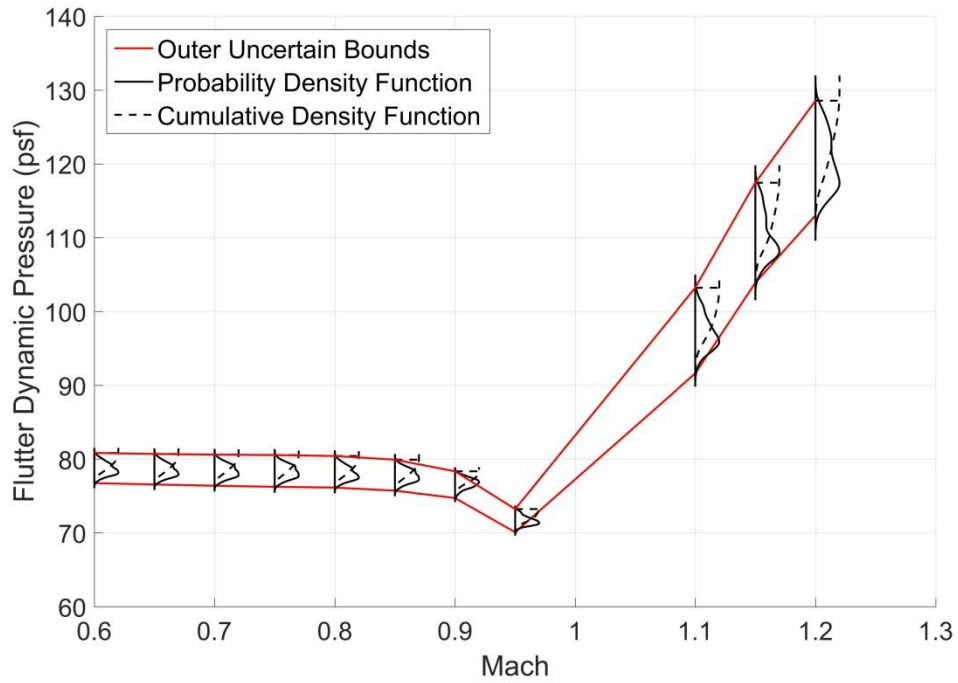


Figure 8: Outer uncertainty bounds and PDF/CDF for flutter dynamic pressure using the SVD based technique.

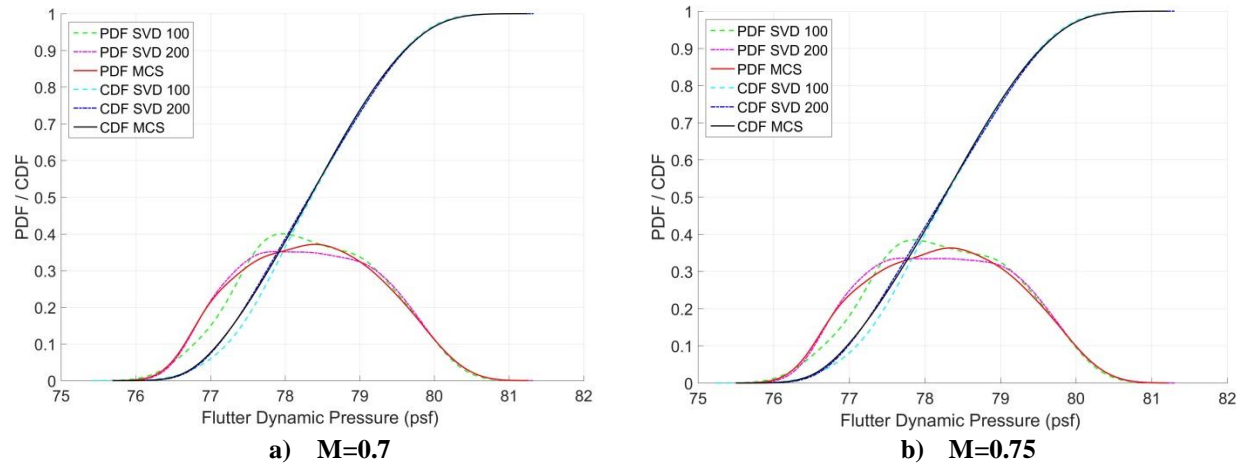


Figure 9: Probability Density Function (PDF) and Cumulative Density Function (CDF) for the flutter pressure dynamic at different Mach numbers (M) obtained using the SVD based method and MCS.

B Probabilistic Results using Monte-Carlo Analysis

The probabilistic analysis of the Semi-Span Super-Sonic Transport vehicle included the execution of a dynamic aeroelastic analysis. The flutter mechanisms of the aeroelastic model were identified for a range of Mach numbers and the corresponding flutter dynamic pressures were calculated. The computationally intensive simulation process was performed efficiently and rapidly on a properly configured computer cluster, leveraging hardware and software resources. Using the parallelization flexibility of the computer cluster, the output responses of the Monte-Carlo analysis, which included 5000 runs, were systematically retrieved during the probabilistic analysis for the selected input variables, namely the fuselage and engine nacelles masses.

The Probability Density Functions for the flutter dynamic pressure of the Semi-Span Super-Sonic Transport vehicle for a range of Mach numbers, obtained from the Monte-Carlo analysis which included 5000 runs, are depicted in Figure 10. In the same diagram, the maximum and minimum probabilistic values of the examined metrics are highlighted (dashed-dotted curves), while the flutter dynamic pressures obtained for the baseline case are also plotted (black dots). Observing Figure 10, it becomes apparent that the probability density function of the metrics is following a relatively narrow normal distribution for subsonic speeds, while for supersonic speeds the distributions of the flutter dynamic pressure are appearing to have higher variation, affecting significantly the predictability for the aeroelastic stability of the vehicle. Additionally, the mean values of the flutter dynamic pressure obtained from the probabilistic analysis (dashed curve) are coinciding with the curve that connects the corresponding deterministic values (solid curve).

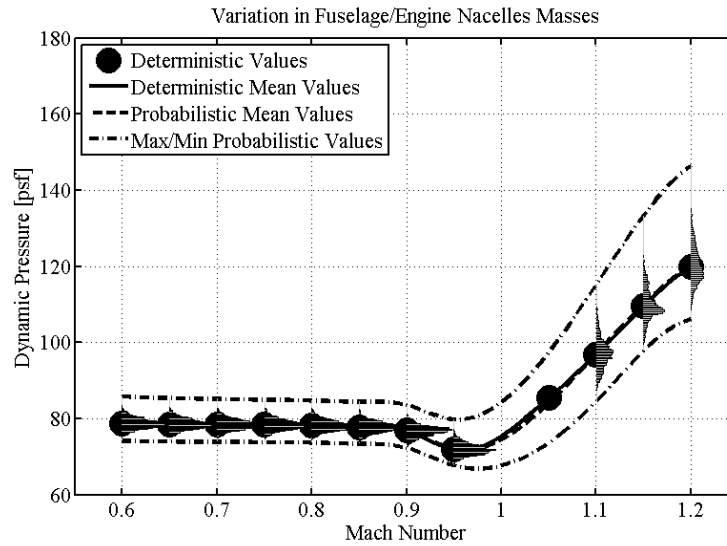


Figure 10. Probability Density Function for the flutter dynamic pressure of the Semi-Span Super-Sonic Transport vehicle for a range of Mach numbers (Monte-Carlo analysis (5000 runs)).

C Probabilistic Results using PCE Analysis

The Polynomial Chaos Expansion method, described above, was used in order to predict the variability of the response functions and the minimum sample size for achieving a satisfying accuracy was identified through a parametric study. In the current study, the mathematical formulation of the PCE method was written and implemented in MATLAB. The uncertain variables were varied following the normal distribution and the Polynomial Chaos Expansion models were created using Hermite polynomials. Different oversampling ratios (sample size/minimum sample size) were investigated, utilizing the Latin Hypercube sampling and the Hammersley sequence, in an effort to monitor convergence and keep the computational cost as low as possible. Indicatively, the root mean square error for the approximation of the flutter dynamic pressure for Mach=0.95 is included in Table 12-5 using 2nd and 3rd order PCE models and various oversampling ratios. It is worth noting that with the 3rd order approximation model, an excellent correlation was achieved for oversampling ratio of 1.2 (Figure 11).

Table 5. Root Mean Square Error for the flutter dynamic pressure (Mach=0.95) using 2nd and 3rd order Polynomial Chaos Expansion models and different oversampling ratios.

| RMSE | Oversampling Ratio | | | | | |
|-------------------------------------|--------------------|--------|--------|--------|--------|--------|
| | 1 | 1.2 | 1.4 | 1.6 | 1.8 | 2 |
| 2 nd Order PCE (Hermite) | 0.5521 | 0.1507 | 0.0875 | 0.0815 | 0.0951 | 0.0795 |
| 3 rd Order PCE (Hermite) | 0.3880 | 0.0521 | 0.0378 | 0.0388 | 0.0319 | 0.0281 |

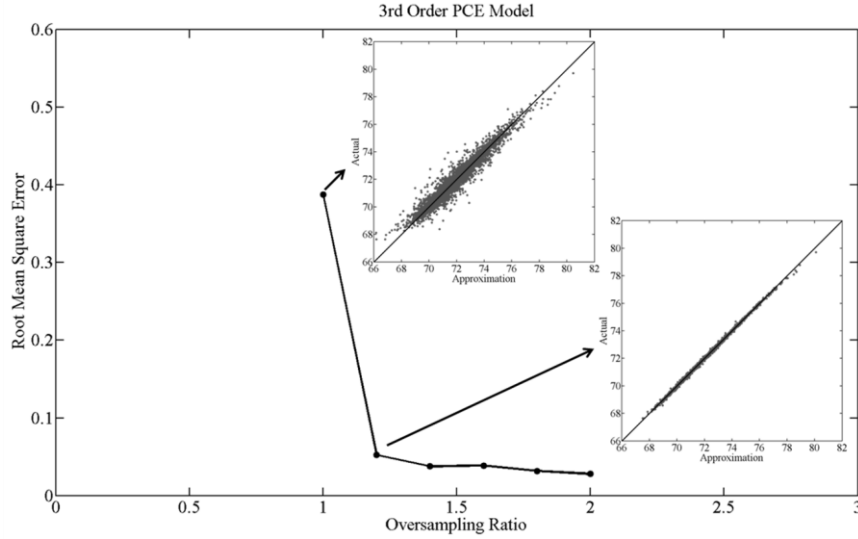


Figure 11. Root Mean Square Error for the flutter dynamic pressure (Mach=0.95) using a 3rd order Polynomial Chaos Expansion model and different oversampling ratios.

Accordingly, the approximated Probability Density Functions of the flutter dynamic pressure for Mach=0.95 derived from 2nd and 3rd order PCE models, created using Hermite polynomials, are depicted in Figure 12(a) and (b) (dashed curve), along with the corresponding results obtained from the Monte-Carlo analysis (solid curve). It becomes apparent that there is a discrepancy between the actual and predicted results for the 2nd order polynomial approximation (Figure 12(a)), while an excellent agreement is observed for the 3rd order model (Figure 12(b)). In Figure 12(c), similar results, obtained from 2nd, 3rd and 4th order PCE models created using Hermite polynomials and Hammersley samples of size 136, 816 and 3876, respectively, are presented. It is worth noting that as the order of the PCE models is increasing, the polynomial approximations are becoming more accurate.

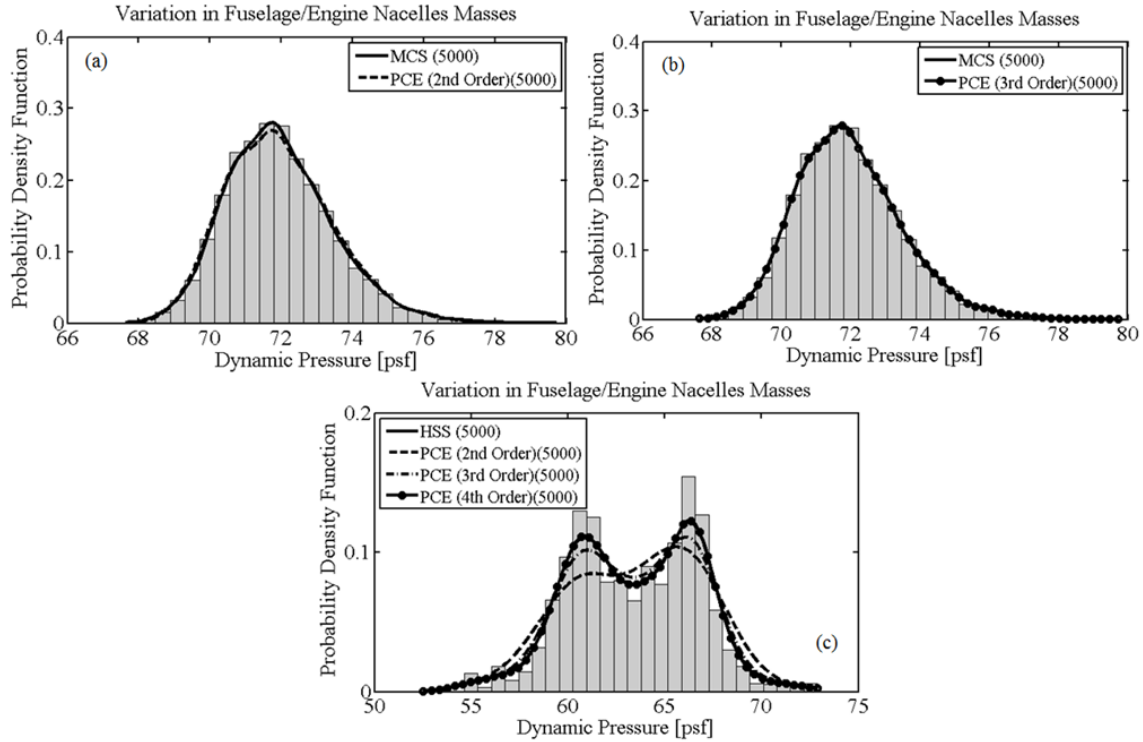


Figure 12. Probability Density Function of the flutter dynamic pressure for Mach number=0.95 obtained using Polynomial Chaos Expansion models of (a) 2nd order and oversampling ratio of 2, (b) 3rd order and oversampling ratio of 1.2 and (c) 2nd, 3rd and 4th order and oversampling ratio of 1.

D Results Using Fuzzy Analysis

The Kriging predictor coupled with the fuzzy analysis, described in this chapter, were used for uncertainty propagation in the flutter analysis of the Semi-Span Super-Sonic Transport vehicle. The functions of the Kriging predictor were written in MATLAB. The variation of the uncertain input parameters is assumed as in the previous test case and their triangular membership function are found according to Eq. (14). The Kriging predictor model is trained with 816 design points (LHS sample), similar to the previous examples, and used for optimisation studies at 21 different α values of the fuzzy membership functions of the input parameters.

Figure 13(a) shows the ranges of variation for the flutter dynamic pressure of the Semi-Span Super-Sonic Transport vehicle versus different Mach numbers, obtained from the fuzzy analysis. The color map in this figure indicates the flutter dynamic pressure for each α value. As it can be seen in the figure the bounds of the flutter dynamic pressures are slightly higher than those obtained from the probabilistic methods (Figure 10). This is due to the fact that the bounds at zero values indicate the maximum possible variations of the flutter dynamic pressure. A similar trend for the variation of the flutter dynamic pressures versus Mach numbers can be observed where the instability bounds in subsonic region are relatively narrower than the corresponding variations for supersonic speeds. Equally, Figure 13(b) shows the fuzzy membership function of the flutter dynamic pressure at Mach=0.95. The maximum variation at zero α value is slightly higher than the corresponding variation obtained from the probabilistic methods (Figure 13(b)). However, as already explained, this is due to the fact that zero α values show maximum possible variations of the dynamic pressure, meaning that there is zero degree of belief that these variations might happen.

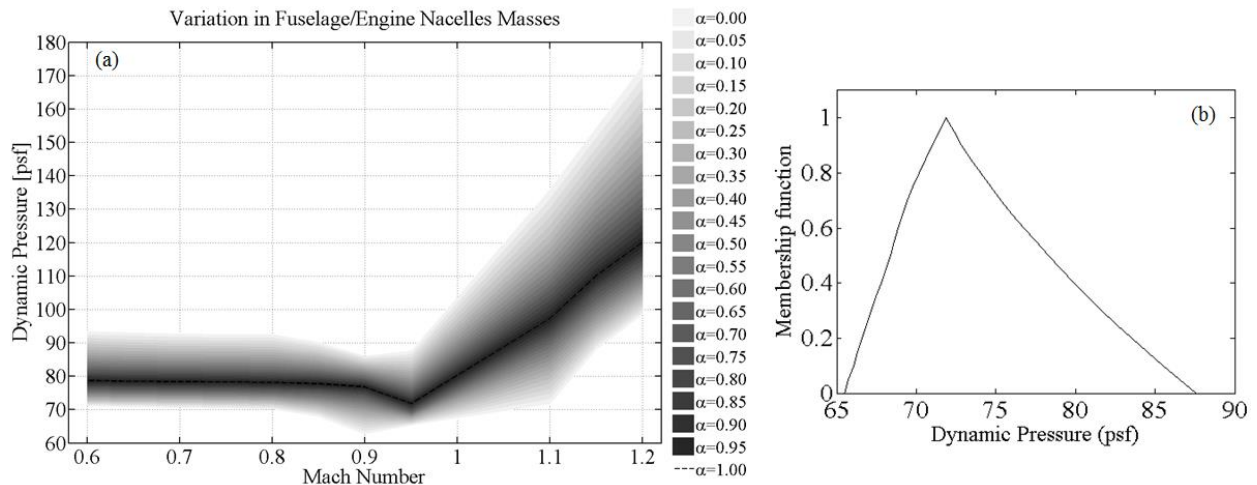


Figure 13. (a) Fuzzy plot of the flutter dynamic pressure in function of Mach number and (b) Fuzzy membership function of flutter dynamic pressure at Mach=0.95.

IV. Conclusions

A Singular Value Decomposition (SVD) based reduced order model technique, Polynomial Chaos Expansion and Fuzzy Logic methods have been applied for the efficient prediction and propagation of uncertainty of flutter dynamic pressure for the S4T supersonic aircraft wind tunnel model. A very high accuracy has been achieved for the prediction of uncertainty bounds compared to Monte Carlo simulations with a significant reduction in computational requirement. Such techniques provide much promise for the investigation of the effects of uncertainty on aeroelastic systems, including determination of the structural parameters that have the most significant effect, leading to the goal of robust design.

V. Acknowledgments

This work is partially supported through the European Community's Marie Curie Initial Training Network (ITN) on Aircraft Loads Prediction using Enhanced Simulation (ALPES) FP7-PEOPLE-ITN-GA-2013-607911, the Royal Academy of Engineering and the Virtual Engineering Centre (VEC). The VEC is a University of Liverpool

initiative in partnership with the Northwest Aerospace Alliance, the Science and Technology Facilities Council (Daresbury Laboratory), BAE Systems, Morson Projects and Airbus (UK). The VEC was catalysed by funding from the Northwest Regional Development Agency (NWDA) and European Regional Development Fund (ERDF) to provide a focal point for virtual engineering research, education and skills development, best practice demonstration, and knowledge transfer to the aerospace sector.

The authors would like also to acknowledge the NATO-S&T Advanced Vehicle Technology research group AVT-191 “Application of Sensitivity Analysis and Uncertainty Quantification to Military Vehicle Design”, for providing the aircraft model used in this study.

References

- [1] W.A. Silva et al, “*An Overview of the Semi-Span Super-Sonic Transport (S4T) Wind-Tunnel Program*”, 53rd AIAA/ASME/ASCE/AHS/ASC Structures, Structural Dynamics, and Materials Conference, AIAA, Honolulu, Hawaii. 2012.
- [2] I. Tartaruga, J. E. Cooper, M. H. Lowenberg, P. Sartor, S. Coggon and Y. Lemmens. “*Prediction and Uncertainty Propagation of Correlated Time-Varying Quantities using Surrogate Models*”. CEAS Aeronautical Journal. DOI 10.1007/s13272-015-0172-1. 2015.
- [3] I. Tartaruga, J. E. Cooper, P. Sartor, M. H. Lowenberg, S. Coggon and Y. Lemmens “*Efficient Prediction and Uncertainty Propagation of Correlated Loads*”. 56th AIAA/ASME/ASCE/AHS/ASC Structure, Structural Dynamics, and Materials Conference, Orlando, Florida USA, January 5-9, 2015.
- [4] I. Tartaruga, J. E. Cooper, M. H. Lowenberg, P. Sartor and Y. Lemmens . “*Probabilistic Bounds for Correlated Aircraft Loads using Geometrical Considerations*”. 13th International Probabilistic Workshop (IPW 2015), Liverpool, UK. 4-6 November 2015.
- [5] I. Tartaruga, J. E. Cooper, M. H. Lowenberg, P. Sartor and Y. Lemmens. “*Geometrical Based Method for the Uncertainty Quantification of Correlated Aircraft Loads*”. Accepted for publication in the Int J Aeroelasticity and Structural Dynamics.
- [6] I. Tartaruga, J. E. Cooper, M. H. Lowenberg, P. Sartor and Y. Lemmens. “*Evaluation and Uncertainty Quantification of Bifurcation Diagram: Landing Gear, a case study*”. Proceeding of UNCECOMP 2015, Crete, Greece. May 25-27 2015
- [7] I. Tartaruga, P. Sartor, J. E. Cooper, M. H. Lowenberg and Y. Lemmens. “*Sensitivity Analysis and Uncertainty Quantification in the presence of Hopf Bifurcations*”. Submitted to SIAM/ASA J. Uncertainty Quantification.
- [8] G. Georgiou, A. Manan and J.E. Cooper. “*Modeling Composite Wing Aeroelastic Behaviour with Uncertain Damage Severity and Material Properties*”. Mechanical Systems and Signal Processing, v32, pp. 32-43. October 2012.
- [9] Manan and J.E. Cooper. “*Design of Composite Wings Including Uncertainties - A Probabilistic Approach*”, Journal of Aircraft, v46, n2, pp. 601-607. 2009.
- [10] K.J. Badcock, H.H. Khodaparast, S. Timme and J.E. Mottershead. “*Calculating the Influence of Structural Uncertainty on Aeroelastic Limit Cycle Response*”. 52nd AIAA/ASME/ASCE/AHS/ASC Structures, Structural Dynamics, and Materials Conference, Denver, Colorado, USA. April 4-8 2011,
- [11] Q. Ouyang, X. Chen and J. E. Cooper. “*Robust Aeroelastic Analysis and Optimization of Composite Wing Under μ -Analysis Framework*”. Journal of Aircraft, v50, pp. 1299-1305. 2013.
- [12] C. Scarth, P. Sartor, J. E. Cooper, P. M. Weaver and G. H. C. Silva. “*Robust Aeroelastic Design of Composite Plate Wings*”. 17th AIAA Non-Deterministic Approaches Conference, Orlando, Florida, USA. January 5-9 2015.
- [13] C. Scarth, J.E. Cooper, P. M. Weaver and G H.C. Silva “*Uncertainty Quantification of Aeroelastic Stability of Composite Plate Wings using Lamination Parameters*” Composite Structures v116 pp 84-93. 2014
- [14] G. Georgiou, J.E. Cooper, D. Hung and A. Mosquera. “*Uncertainty quantification of the Aeroelastic Behavior of a supersonic vehicle using an engineering cloud*”. Proceedings of ISMA2012-USD2012, pp. 4559-4573. 2012.
- [15] G.Georgiou, H.H.Khodaparast and J.E.Cooper “*Uncertainty Quantification of Aeroelastic Stability*” – Chapter 16 in Mathematics of Uncertainty Modeling in the Analysis of Engineering and Science Problems. Pub IGI Global DOI: 10.4018/978-1-4666-4991-0.ch016 2014

- [16] W.P. Rodden and E.H. Johnson, *MSC.Nastran Aeroelastic Analysis User's Guide* v68, The MacNeal-Schwendler Corporation 1994.
- [17] <http://www.robots.ox.ac.uk/~mebden/reports/GPtutorial.pdf>, last access December 2015.
- [18] J.D. Martin and T.W. Simpson “On the use of Kriging Models to approximate deterministic computer models”, in Proceedings of DETC’04: ASME 2004 International Design Engineering Technical Conference and Computer and Information in Engineering Conference, Salt Lake City, Utah USA, September 28 – October 2, 2004.
- [19] N. Wiener. “*The Homogenous Chaos*” American Journal of Mathematics. 60(4) pp 897 – 936 1938
- [20] K. Ito. “*Multiple Weiner Integrals*” J. Mathematical Society of Japan. V3 pp157 – 169. 1951
- [21] R.G. Ghanem & P.D. Spanos. “*Stochastic Finite Elements: A Spectral Approach*” Springer-Verlag 1991.
- [22] L.A. Zadeh. “*Fuzzy Sets*”. Information and Control 8(3) pp 338 – 353 1965
- [23] M. Hanns, “*The Transformation Method for the Simulation and Analysis of Systems with Uncertain Parameters*” Fuzzy Sets and Systems 130(3). pp 279-289 2002
- [24] H.J. Zimmermann, “*Fuzzy Set Theory and its Applications*” 4th ed Kluwer 2001.
- [25] D.J. Dubois & H.Prade, “*Fuzzy Sets and Systems – Theory and Applications*” Mathematics in Science and Engineering v144. Academic Press. 1980
- [26] D. Moens & D. Vandepitte, “A Survey of Non-Probabilistic Uncertainty Treatment in Finite Element Analysis” Computer Methods in Applied Mechanics and Engineering 194(12-16) pp 1527 – 1555. 2005
- [27] D. Moens & D. Vandepitte, “Recent Advances in Non-Probabilistic Approaches for Non-Deterministic Dynamic Finite Element Analysis” Archives of Computational Methods in Engineering 13(3) pp 389 – 464 2006
- [28] S. Lapointe & B Bobee, “Revision of Possibility Distribution: A Bayesian Inference Pattern” Fuzzy Sets and Systems 116(2) pp119-140. 2000
- [29] D.J. Dubois & H. Prade, “A Review of Fuzzy Set Aggregation Connectives” Information Sciences 36(1-2) pp 1080 – 1092. 1985
- [30] M. Hanss & K. Willner, “A Fuzzy Arithmetical Approach to the Solution of Finite Element Problems with Uncertainty Parameters” Mechanics Research Communications 27(3) pp257-272. 2000
- [31] R.E. Moore, “*Interval Analysis*” Prentice-Hall. 1966
- [32] G. Manson, “Calculating Frequency Response Functions for Uncertain Systems using Complex Affine Analysis” J. Sound and Vibration 288(3) pp 487-521 2005
- [33] D. Degrauwe, G. Lombaert & G de Roeck, “Improving Interval Analysis in Finite Element Calculations by Means of Affine Arithmetic” Computers & Structures 88(3-4) pp 247 – 254. 2010
- [34] M. DeMunck, D. Moens, W. Desmet and D. Vandepitte, “An Efficient Response Surface Based Optimization Method for Non-Deterministic Harmonic and Transient Dynamic Analysis” Computer Modelling in Engineering and Sciences 47(2) 2009 pp119-166. 2009
- [35] B. Lallemand, G Plessis, T.Tison and P.Level, “Neumann Expansion for Fuzzy Finite Element Analysis” Engineering Computations 16(5) pp 572 – 583. 1999
- [36] O. Giannini & M Hanss, “The Component Mode Transformation Method: A Fast Implementation of Fuzzy Arithmetic for Uncertainty Management in Structural Dynamics” J. Sound and Vibration 311(3-5) pp1340-1357. 2005
- [37] U. Gauger, S. Turrin, M. Hanss & L. Gaul, “A New Uncertainty Analysis for the Transformation Method” Fuzzy Sets and Systems 159(11) pp. 1273-1291. 2008
- [38] M. DeMunck, D. Moens, W. Desmet & D. Vandepitte, “A Response Surface Based Optimization Algorithm for the Calculation of Fuzzy Envelope FRFs of Models with Uncertain Properties” Computers and Structures 86(10) pp1080-1092 2008
- [39] H.H. Khodaparast, J.E.Mottershead & K.J. Badcock, “Propagation of Structural Uncertainty to Linear Aeroelastic Stability” Computers & Structures 88(3-4) pp223-236. 2010
- [40] M Hanss, “*Applied Fuzzy Arithmetic : An Introduction with Engineering Applications*” Springer-Verlag. 2005.